Dalton
Transactions

Cite this: *Dalton Trans.*, 2012, **41**, 11813

www.rsc.org/dalton

PAPER

Photoswitchable electrochemical behaviour of a [FeFe] hydrogenase model with a dithienylethene derivative†

Hui-Min Wen, Jin-Yun Wang, Ming-Qiang Hu, Bin Li, Zhong-Ning Chen* and Chang-Neng Chen*

Received 9th July 2012, Accepted 2nd August 2012
DOI: 10.1039/c2dt31507f

A diiron dithiolate complex **1o** with a dithienylethene (DTE) phosphine ligand has been elaborately designed and fully investigated by spectroscopic and DFT computational studies. Upon irradiation with UV light, the DTE moiety in complex **1o** undergoes an excellent photocyclization reaction to attain ring-closed state **1c** in high yield (>95%), accompanied by a colour change from orange to deep blue. On the other hand, upon irradiation with visible light (>460 nm), ring-closed form **1c** in CH_3CN solution reverts perfectly into ring-open form **1o**. Both **1o** and **1c** were characterised by IR, ^1H, ^{31}P, ^{19}F NMR and electrochemical spectroscopy. The electrochemical behaviours of both the open and closed forms were investigated by cyclic voltammetry. Upon photocyclization reaction, a 290 mV (from −2.29 V to −2.00 V) positive shift is induced in the potential of electrochemical catalytic proton reduction, due to the electron-withdrawing effect of the ring-closed DTE moiety. Consequently, complex **1** can reversibly photoswitch the potential of proton reduction on the [FeFe] moiety.

Introduction

Hydrogen gas is regarded as a promising clean and renewable energy source for the future. [FeFe] hydrogenase has received intensive attention because of its high efficiency in reversible H_2 production and/or H_2 oxidation in nature under mild conditions: $2H^+ + 2e \rightleftarrows H_2$ [1]. The X-ray crystallographic analyses of the [FeFe] hydrogenase enzymes from *Desulfovibrio desulfuricans* Hildenborough and *Clostridium pasteurianum* I have revealed that the active site is a novel dithiolate bridged di-iron cluster which shares a structural resemblance with the di-iron dithiolate carbonyl organometallic complexes.[2] In order to mimic the structure and behavior of the active site, extensive researches have been devoted to find catalyst candidates for biomimetic hydrogen production and uptake. In the past decades, numerous catalyst models based on [2Fe2S] complexes have been synthesized, and most of them have shown inspiring electrocatalytic[3,4] and photocatalytic activities.[5,6] Generally, the most economical catalysts are supposed to be those having a low reduction potential and a remarkable increase in the intensity of the reduction current with the addition of acid.[8] Recently, the di-iron complex with a less negative reduction potential is highlighted for photo-catalytic hydrogen production, because the reduction potential of the dinuclear iron complex needs to be more positive than that of the excited state of the photosensitizer, making the photoinduced electron transfer from the photosensitizer to the catalyst thermodynamically feasible.[5–7] Today, one of the most prominent ways to reduce the reduction potential is to introduce electron-withdrawing chloro substituents onto the dithiolate bridge of diiron dithiolate hexacarbonyl complexes, as reported by Ott and co-workers.[9] Sun *et al.* reported another approach to adjust the reduction potentials and improve the photostability of the [2Fe2S] model complexes by using weak electron donating phosphine ligands to displace carbonyls.[10] We report herein a novel [2Fe2S] model compound to tune the potential of hydrogen production by introducing a photochromic dithienylethene (DTE) unit into the [FeFe] hydrogenase subsite mimic.

As we know, the combination of the photochromic ligands with other functional systems can change reversibly not only the absorption spectra, but also their geometrical and electronic structures,[11] which eventually switch the physicochemical properties such as fluorescence, electrical conductivity and magnetism.[12,13] Since dithienylethenes (DTEs) are a class of efficient photochromic compounds because of their excellent photochromic properties such as fast response, fatigue resistance and facile color-control,[11–12] they can undergo a reversible change between the ring-open and ring-closed states upon irradiation with proper UV/Vis light, resulting in the conversion of both the color and the electronic structure of the whole molecule. Considering that the ring-closed isomer of the DTE moiety is a stronger π-electron accepter than its ring-open counterpart,[13,14] it is expected that the incorporation of a dithienylethene ligand into the [FeFe] hydrogenase model would modulate the reduction potential of the [FeFe] moiety. In order to achieve this target, we elaborately designed and prepared compound **1o** (Scheme 1) that

---

State Key Laboratory of Structural Chemistry, Fujian Institute of Research on the Structure of Matter, Chinese Academy of Sciences, Fuzhou, Fujian 350002, China. E-mail: ccn@fjirsm.ac.cn; Tel: (+86) 591-8379-2395

† Electronic supplementary information (ESI) available: Spectral data; optimized geometries; and computational details. See DOI: 10.1039/c2dt31507f

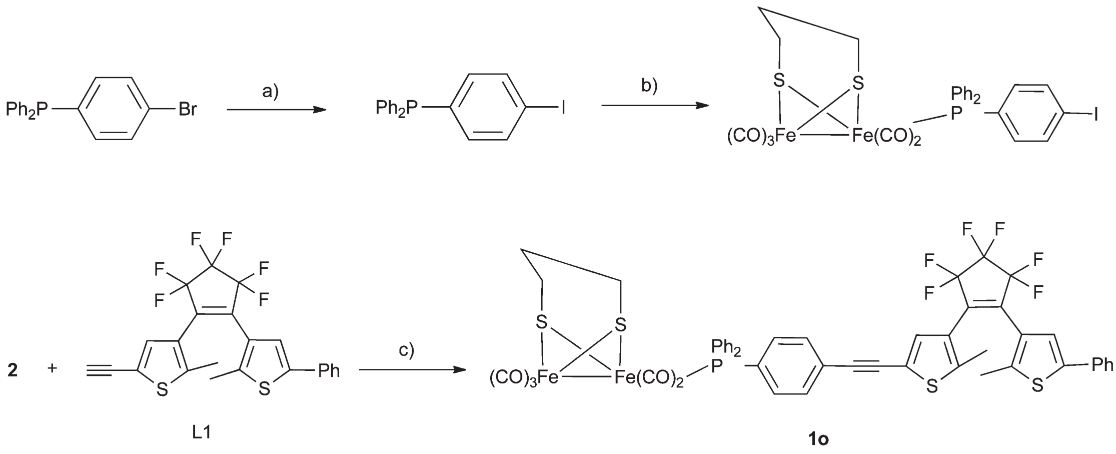

Scheme 1 Synthetic routes to **1o**. (a) (i) *n*-BuLi, THF; (ii) I_2; (b) (μ-pdt)$Fe_2(CO)_6$, $Me_3NO·2H_2O$, CH_3CN; (c) [$PdCl_2(PPh_3)_2$], CuI, TEA, toluene, 40 °C.

incorporated the dithienylethenederivative L1 into the [FeFe] hydrogenase model.[15]

Results and discussion

Synthesis and characterization

Ott and co-workers have synthesized a dyad in which the photosensitizer was linked to a model of the [FeFe] hydrogenase active site by a phosphine ligand.[15] We chose a similar phosphine ligand to prepare complex **1** by reaction of L1 (1-(5-methyl-2-(2-phenyl)-4-thienyl)-2-(2-methyl-5-ethynyl-3-thienyl)-perfluorocyclopentene) with the complex **2** [(μ-pdt)$Fe_2(CO)_5$-($PPh_2C_6H_4I$-4)] (pdt = propanedithiolate = –$SCH_2CH_2CH_2S$–) moiety through Sonogashira cross coupling reaction in the presence of $Pd(PPh_3)_2Cl_2$ and CuI in TEA–toluene solution (Scheme 1). The IR spectrum of complex **1o** in CH_3CN exhibits three major bands in the CO region at 2044, 1984, 1931 cm^{-1}, which is comparable to that of triphenylphosphine monosubstituted di-iron dithiolate complexes, indicating similar skeletal and electronic structures for these complexes.[15] After the photocyclization reaction, no distinguishable shift is observed in **1c**.

The photochromic reaction has been monitored by ^1H, ^{31}P and ^{19}F NMR spectra in CD_2Cl_2.[16] Upon irradiation with UV light, the two thienyl proton signals of **1o** at 7.30 (H_{1o}) and 7.26 (H_{2o}) ppm show a high field shift to 6.69 (H_{1c}) and 6.51 (H_{2c}) ppm due to the formation of the ring-closed form **1c**, indicating a higher electron density in both DTE thiophene rings than in the ring-open counterparts (Fig. 1a).[16] The ^{31}P NMR signal of the open form **1o** at 65.06 ppm is shifted slightly to the low-field at 65.38 ppm in the closed form (Fig. 1b).[16] In the ^{19}F NMR spectra, the open form **1o** exhibits one signal at −132.2 ppm, two signals at −110.3 and −110.4 ppm with an intensity ratio of 1 : 1 : 1 (Fig. S1†).[16] Upon photocyclization, the signal at −132.2 ppm is gradually reduced, a high-field shifted signal is observed at −133.8 ppm due to the conversion of **1o** → **1c**. Meanwhile, the two signals at −110.3 and −110.4 ppm are progressively decreased, whereas four sets of doublets are detected at high-field from −112.0 to −115.1 ppm, indicating higher electron density in DTE perfluorocyclopentene after photocyclization (Fig. S1†).[14] The conversion percentage of **1o** → **1c** at the photostationary state (PSS) is >95%, as revealed from ^1H, ^{31}P and ^{19}F NMR spectral studies.

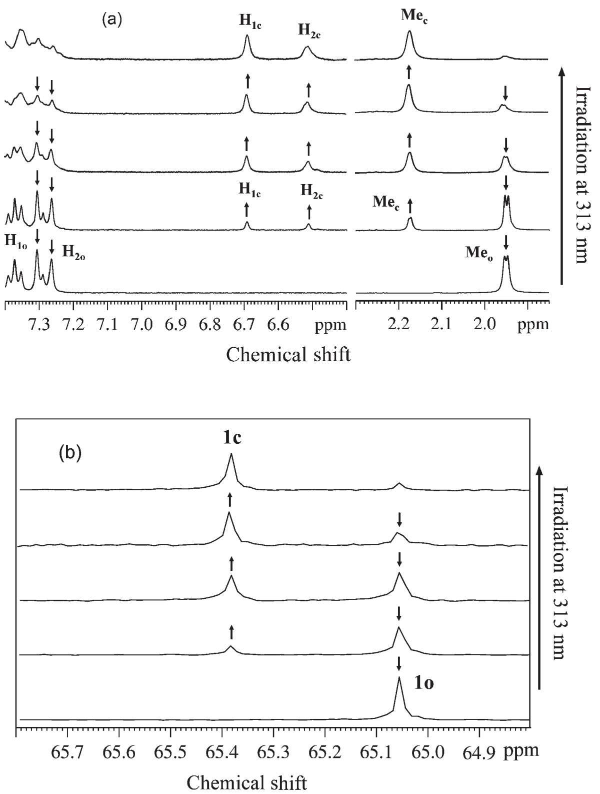

Fig. 1 The (a) ^1H and (b) ^{31}P NMR spectral changes of **1o** in CD_2Cl_2 upon irradiation with 313 nm, showing the conversion of **1o** → **1c**.

Electronic absorption and photochromic properties

Photochromic conversions of complex **1** are depicted in Scheme 2. Upon irradiation at 313 nm within 80 s, **1o** in

CH_3CN turns from orange to deep blue (Scheme 2), followed by the UV-Vis absorption spectral changes (Fig. 2). The absorption bands of ring-open **1o** in CH_3CN are located at 271 nm and 321 nm. Based on the TD-DFT calculations, the high-energy absorption band at 271 nm is mainly composed of IL [$\pi \rightarrow \pi^*$(DTE)] intraligand transition and CLCT [3d(Fe) → π^*(DTE)] clusters to ligand charge transfer transition (Table 1). The absorption at 321 nm is primarily ascribed to the intracluster transitions (IC) within the Fe_2S_2 cluster mixed with some IL [$\pi \rightarrow \pi^*$(DTE)] character based on TD-DFT calculations (Table 1).

Upon irradiation at 313 nm, the two intense UV absorptions gradually decrease, while two new absorption bands at 380 nm and 600 nm appear due to the photocyclization reaction of **1o** to **1c** (Fig. 2a). The shoulder peak at 380 nm of the closed form **1c** arises from IC transition of the Fe_2S_2 cluster mixed with some CLCT charge transfer transition from Fe_2S_2 cluster to $PPh_2PhC{\equiv}C$/DTE (Table 2). The low energy absorption at 600 nm is mainly contributed by the IL [$\pi \rightarrow \pi^*$(DTE)] transition of the ring-closed isomer. On the other hand, upon irradiation with visible light (>460 nm) for 12 min, ring-closed complex **1c** in CH_3CN solution reverts into the open form (Fig. 2b). As shown in Fig. S2,† this complex shows excellent reversibility in its photochromic behavior, with no apparent loss in its photochromic reactivities over at least six repeating cycles. The quantum yields for the photocyclization and photocycloreversion of the complex are 0.45 ($\Phi_{o\text{-}c}$) and 0.017 ($\Phi_{c\text{-}o}$) respectively.

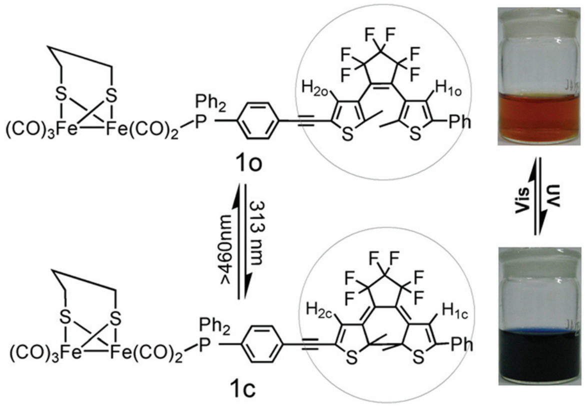

Scheme 2 Photochromic behaviour of complex **1**.

Electrochemistry

The cyclic voltammograms (CV) of **1o** and **1c** were monitored under N_2 with stepwise addition of HOAc in CH_3CN solution. Complex **1o** exhibits two obvious irreversible reductive peaks at −1.78 and −1.95 V in the absence of HAcO *vs.* Fc–Fc$^+$. The first irreversible reduction at −1.78 V due to the diiron portion is quite similar to PPh_3 mono-substituted complexes.[15] With reference to previous works on many phosphine ligand mono-substituted diiron analogues, the first reduction is assigned to [Fe^IFe^I] → [Fe^IFe^0].[17,18] Controlled-potential electrolysis of complex **1o** (1 mM in the absence of acid in CH_3CN at −1.45 V *vs.* Ag/AgCl ≈ −1.85 V *vs.* Fc$^+$–Fc) requires a net consumption of about 0.9 F mol^{-1}, which supports the assignment of the one-electron reduction process under these conditions. As a result, the one-electron reduced product could be unambiguously

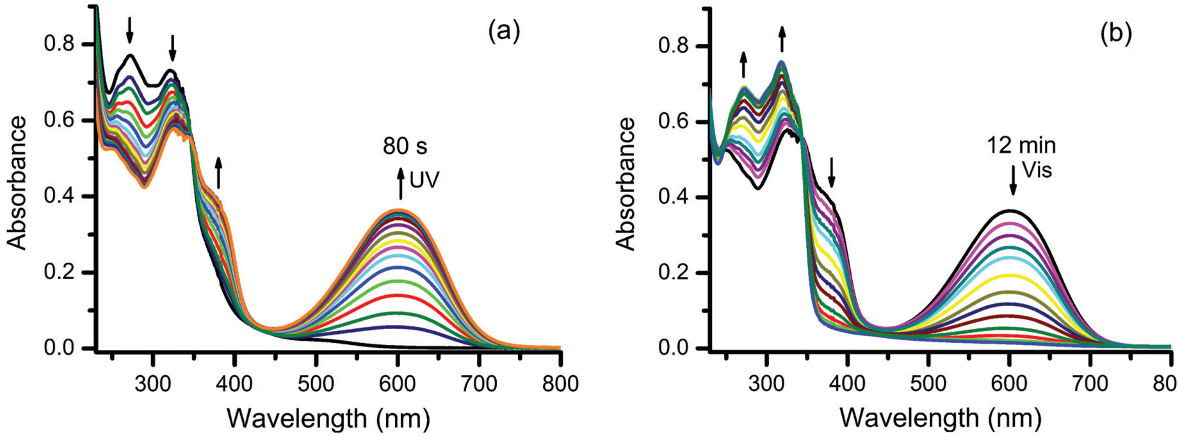

Fig. 2 (a) The UV-Vis absorption spectral changes of the complex **1o** (2×10^{-5} M) in CH_3CN at 298 K upon irradiation at 313 nm. (b) The UV-Vis absorption spectral changes of the complex **1c** (2×10^{-5} M) in CH_3CN at 298 K upon irradiation at >460 nm.

Table 1 Absorption transitions and singlet excited states for **1o** in CH_3CN, calculated by TD-DFT method

	E/nm (eV)	Transition	Contrib. (%)	O.S.	Assignment	Exp./nm
S_{13}	342.89 (3.62)	HOMO → LUMO + 2	35.80	0.7568	IC/IL	321
		HOMO − 1 → LUMO + 1	28.62		IL/IC/CLCT/LLCT	
		HOMO → LUMO	25.30		IC/IL/CLCT	
S_{31}	283.79 (4.37)	HOMO − 1 → LUMO + 3	47.42	0.3965	IL/CLCT/LLCT	271
		HOMO → LUMO + 3	37.76		CLCT/IL/LLCT	

Table 2 Absorption transitions and singlet excited states for **1c** in CH_3CN, calculated by TD-DFT method

	E, nm (eV)	Transition	Contrib. (%)	O.S.	Assignment	Exp (nm)
S_1	641.90 (1.93)	HOMO → LUMO	79.51	0.6272	IL	600
S_7	387.74 (3.20)	HOMO − 1 → LUMO + 1	34.24	0.3472	IC/CLCT/IL	380 Sh
		HOMO → LUMO + 1		0.2615	LCCT/IL/LLCT	

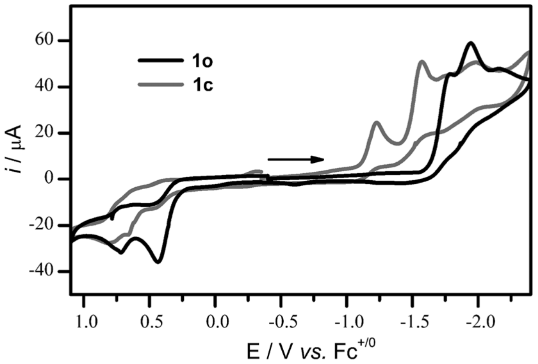

Fig. 3 Cyclic voltammograms of complex **1o** (black line) and **1c** (gray line), 1.0 mM in 0.1 M ^{n}Bu$_4$NPF$_6$–CH_3CN at a scan rate of 100 mV s^{-1} *vs.* Fc^+–Fc.

observed in electrochemistry as that described in the previous literature.[10,18–23] The middle peak at −1.95 V exhibits a slightly positive shift compared to that of free ligand L1o (E_{red} = −2.03 V), implying that this reduction process is localized on the DTE unit (Fig. 3). In the presence of HOAc, a new reduction peak at −2.29 V is involved in electrocatalysis of H_2 production as evidenced by the increase in current with acid concentration (Fig. 4a). This electrocatalytic behavior of **1o** is comparable to the typical electrocatalytic reduction of weak acid in the phosphine ligand mono-substituted or all-carbonyl diiron models (Table 3).[18,22,23]

When the solution of complex **1o** without acid was irradiated by a UV lamp, the reduction wave due to the ring-open DTE moiety at −1.95 V converts to two new reduction peaks at −1.23 and −1.55 V (Fig. 3) with the conversion of **1o** to **1c**. The reductive potential of **1o** at −1.78 V shifts slightly to −1.75 V after photocyclization, which is similar to other aryl phosphine mono-substituted complexes (Fig. S3†).[10,15] On the other hand, the wave (−2.29 V in **1o**) involved in the electrocatalytic proton reduction process is shifted to the less negative region at −2.00 V upon photo-induced ring closure (Fig. 4b), possibly with the same electrocatalytic mechanism as **1o** because of their similar molecular structure and voltammograms. Consequently, 290 mV (from −2.29 V to −2.00 V) positive shift is achieved for the hydrogen production through photocyclization, because the ring-closed DTE is a stronger π-acid than its ring-open counterpart which draws more electron density *via* backbonding from diiron dithiolate cluster.[13,14] Nevertheless, the electrocatalytic efficiency is apparently reduced as concluded from the process that the catalytic current is less sensitive to $[H^+]$ (Fig. S4†). To investigate the stability of the system, the electrochemical behaviour of complex **1** in CH_3CN with 10 equivalents of acetic acid was monitored under repeated irradiation with UV and visible light by cyclic voltammetry, and the cyclic voltammograms can revert between the two states over at least four repeating cycles in 12 h (Fig. S5†).

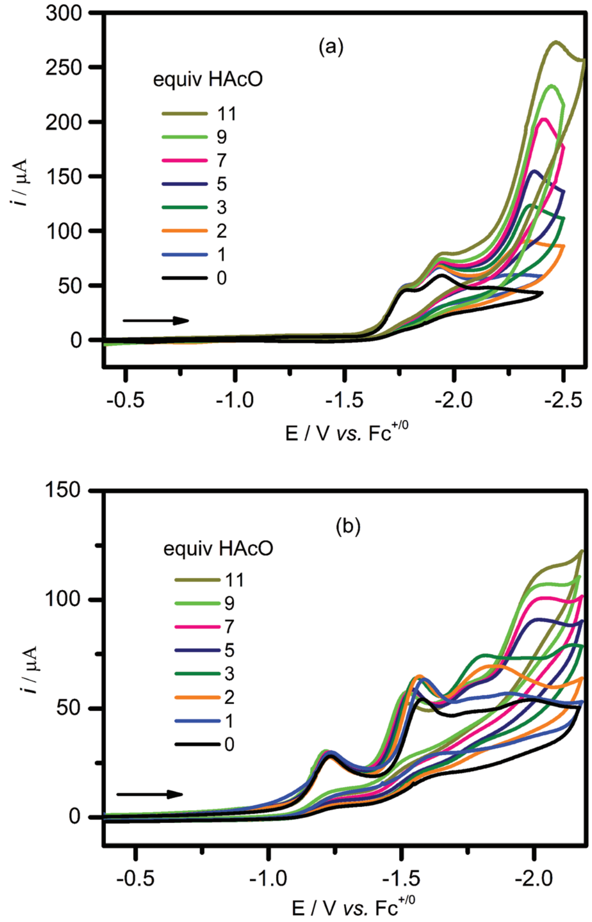

Fig. 4 Cyclic voltammograms of **1o** (a) and **1c** (b), 1.0 mM in 0.1 M ^{n}Bu$_4$NPF$_6$–CH_3CN at a scan rate of 100 mV s^{-1} *vs.* Fc^+–Fc, upon addition of HOAc (0–11 mM).

Table 3 The electrochemical data of L1o, L1c, **1o** and **1c**

	E_{red} [a]/V		
	DTE	Fe_2S_2 center[b]	Fe_2S_2 center[c]
L1o	−2.03	—	—
L1c	−1.30, −1.65	—	—
1o	−1.95	−1.78	−2.29
1c	−1.23, −1.55	−1.75	−2.00

[a] All potentials were recorded in 1.0 mM in 0.1 M ^{n}Bu$_4$NPF$_6$–CH_3CN at a scan rate of 100 mV s^{-1} *vs.* Fc^+–Fc. [b] The reduction potential of $[Fe^IFe^I] \rightarrow [Fe^IFe^0]$. [c] The potential of hydrogen production.

Conclusion

We report for the first time a fairly photo-stable model of iron-only hydrogenases with a photochromic dithienylethene–phosphine ligand. The UV-Vis absorptions of **1** are ascribed reasonably, based on DFT calculation. The electrochemical catalytic proton reduction behavior of the open and closed forms have been investigated, both of which show electrocatalytic hydrogen production. The reductive potential of H_2 production shows a 290 mV anodic shift compared with that of the ring-open form due to the electron-withdrawing performance of the ring-closed DTE moiety upon photocyclization reaction. Consequently, the potential of hydrogen production can be photoswitchable in one molecular system by irradiation with UV/Vis, based on the fact that the distribution of electron density is altered between the ring-open and closed states.

Experimental section

General procedures and materials

All reactions were carried out under a dry argon atmosphere by using Schlenk techniques and vacuum-line systems unless otherwise specified. The solvents were dried, distilled, and degassed prior to use except that those for spectroscopic measurements were of spectroscopic grade. The ligands L1o,[24] (4-bromophenyl)diphenylphosphine[25] and (μ-pdt)$Fe_2(CO)_6$ [26] were prepared by the synthetic procedures described in the literature. Other chemicals were purchased from commercial sources and used without further purification.

Synthesis

PPh_2(*p*-C_6H_4I). To an anhydrous THF (30 mL) solution of (4-bromophenyl)diphenylphosphine (0.512 g, 1.5 mmol) was slowly added *n*-BuLi (1.6 M in hexane, 1.0 mL, 1.6 mmol) using a syringe. After reaction, the mixture was stirred for 40 min at −78 °C and a solution of iodine (0.5 g, 2 mmol) in anhydrous THF (10 mL) was transferred into the reaction flask. The reaction mixture was slowly warmed to room temperature with stirring over 16 h before being quenched by the slow addition of a 10 wt% solution of aqueous sodium sulfite (50 mL). The aqueous layer was separated from the organic layer and extracted with CH_2Cl_2 (3 × 50 mL). The combined organic fractions were washed with brine (50 mL), dried over $MgSO_4$, filtered and evaporated to dryness under reduced pressure. The residue was purified by crystallization from ethanol–water to give PPh_2(*p*-C_6H_4I) (332 mg, 57%) as a colorless solid. ^1H NMR ($CDCl_3$, ppm): 7.00–7.04 (t, 2H, *J* = 7.64 Hz), 7.28–7.36 (m, 10H), 7.65–7.67 (d, 2H, *J* = 7.88 Hz). ^{31}P NMR ($CDCl_3$, ppm): −6.36. ESI-MS (*m*/*z*): 389 $[M + H]^+$.

(μ-pdt)$Fe_2(CO)_5\{PPh_2$(*p*-$C_6H_4I)\}$ (2). A solution of (μ-pdt) $Fe_2(CO)_6$ (0.389 g, 0.5 mmol) and $Me_3NO{\cdot}2H_2O$ (0.111 g, 1 mmol) in CH_3CN (30 mL) was stirred for 5 to 10 min at room temperature. A solution of PPh_2(*p*-C_6H_4I) (0.388 g, 0.5 mmol) in CH_3CN (10 mL) was then added with stirring for 3 h. The solvent was evaporated, and the residue was purified by chromatography on a silica gel column with CH_2Cl_2–hexane (2 : 1 v/v) as the eluent to give **2** (252 mg, 67%) as a dark-red solid. ^1H NMR ($CDCl_3$, ppm): 1.37–1.53 (m, 4H), 1.73–1.78 (m, 2H), 7.38–7.44 (m, 8H), 7.64–7.68 (m, 4H), 7.77 ppm (d, *J* = 7.56Hz, 2H). ^{31}P NMR ($CDCl_3$, ppm): 65.01. ESI-MS (*m*/*z*): 634.7 $[M - 4CO + H]^+$. Elemental analysis calcd (%) for $C_{26}H_20Fe_2IO_5PS_2$: C, 41.85; H, 2.70. Found: C, 41.88; H, 2.63. IR (CH_3CN, cm^{-1}): 2046, 1984, 1931.

1o. [$PdCl_2(PPh_3)_2$] (23 mg, 0.032 mmol) and CuI (2.5 mg, 0.0125 mmol) were added to a degassed solution of [(μ-pdt)-$Fe_2(CO)_5\{PPh_2$(*p*-$C_6H_4I)\}$] (240 mg, 0.32 mmol) and L1o (150 mg, 0.32 mmol) in triethylamine–toluene (1 : 1, 20 mL) solution at 40 °C. After stirring in the dark for 3 h at this temperature, the solution was concentrated *in vacuo* and the black residue was subjected to column chromatography using CH_2Cl_2–hexane (2 : 1 v/v) to give **1o** (146 mg, yield: 42%) as a dark-red solid. ^1H NMR (CD_2Cl_2, ppm): 1.41–1.51 (m, 4H, CH_2), 1.72–1.77 (m, 2H, CH_2), 1.94 (s, 3H, Me), 1.95 (s, 3H, Me), 7.26 (s, 1H, thiophene), 7.27–7.31 (m, 1H, Ph), 7.31 (s, 1H, thiophene), 7.37 (t, 2H, *J* = 7.48 Hz, Ph), 7.46 (m, 6H, Ph), 7.54 (d, 4H, *J* = 7.48 Hz, Ph), 7.62–7.70 (m, 6H, Ph). ^{31}P NMR (CD_2Cl_2, ppm): 65.06. ^{19}F NMR (CD_2Cl_2, ppm): −110.3 (s, 2F), −110.4 (s, 2F), −132.2 (s, 2F). ESI-MS (*m*/*z*) 1031 $[M - 2CO + H]^+$. Elemental analysis calcd (%) for $C_{49}H_{33}F_6Fe_2O_5PS_4$: C, 54.16; H, 3.06. Found: C, 55.21; H, 3.12. IR (CH_3CN, cm^{-1}): 2044, 1984, 1931.

Physical measurements

^1H, ^{31}P and ^{19}F NMR spectra were performed on a Bruker Avance III (400 MHz) spectrometer with $SiMe_4$ as the internal reference and H_3PO_4 as the external reference, respectively. UV-Vis absorption spectra were measured on a Perkin-Elmer Lambda 25 UV-Vis spectrophotometer. Infrared spectra (IR) in CH_3CN solution were recorded on a Magna 750 FT-IR spectrophotometer. Elemental analyses (C, H and N) were carried out on a Perkin-Elmer model 240 C elemental analyzer. Electrospray ionization mass spectrometry (ESI-MS) was recorded on a Finnigan DECAX-30000 LCQ mass spectrometer using dichloromethane as the mobile phase. Cyclic voltammetry (CV) and differential pulse voltammetry (DPV) were conducted with a potentiostat/galvanostat model 263A in acetonitrile solution containing 0.1 M $^nBu_4NPF_6$ as the supporting electrolyte under N_2 unless otherwise stated. DPV was performed at a rate of 20 mV s^{-1} with a pulse height of 40 mV. Platinum and glassy graphite were used as the counter and working electrodes, respectively, and the potential was measured against the Ag/AgCl reference electrode and reported relative to the internal reference of $Fc–Fc^+ = 0.00$ V. UV light was irradiated using a ZF5 UV lamp (313 nm), and visible light irradiation (>460 nm) was carried out by using a LZG220 V500 W tungsten lamp with cutoff filters. The quantum yields were determined by comparing the reaction yields of the diarylethenes against 1,2-bis(2-methyl-5-phenyl-3-thienyl) perfluorocyclo-pentene.[27]

Theoretical methodology

The geometrical structures of compounds **1o** and **1c** as isolated molecules in vacuum were optimized by density functional theory (DFT)[28] methods at the gradient-corrected correlation functional PBE1PBE level.[29] During the optimization processes, the convergent values of maximum force, root-mean-square (RMS) force, maximum displacement, and RMS displacement were set by default. To analyze the spectroscopic properties, eighty simple excited states of the studied compounds were calculated by time-dependent DFT (TD-DFT) methods[30] at the PBE1PBE level on the basis of the optimized geometrical structures. The polarizable continuum model method (PCM)[31] using acetonitrile as the solvent was employed. The self-consistent field (SCF) convergence criteria of the RMS density matrix and maximum density matrix were set at 10^{-8} and 10^{-6} a.u., respectively, in all the electronic structure calculations. The iterations of excited states continued until the changes on energies of states were no more than 10^{-7} a.u. between the iterations, and then convergence was reached in all the excited states. In these calculations, the SDD[32] basis set consisting the effective core potentials (ECP) was employed for the iron, phosphorus, and sulfur atoms, and the 6-31G(p,d)[33] basis set for the remaining atoms were used. To describe precisely the molecular properties, one additional f-type polarization function was implemented for iron (α_f = 2.462) atom,[34] and the d-type polarization function was implemented for phosphorus (α_d = 0.34), and sulfur (α_d = 0.421) atoms.[35] All calculations were performed with the Gaussian 03 program package.[36] Visualization of the optimized structures and frontier molecular orbitals were performed by GaussView. The Ros & Schuit method[37] (C-squared population analysis method, SCPA) is used to partition orbital composition.

Acknowledgements

We thank financial support from the National Natural Science Foundation China (Grant Nos. 20973172, 21071145 and 21101153), the National Basic Research Program of China (no. 2009CB220009), and the Provincial Natural Science Foundation of Fujian (no. 2011J01063).

References

1 M. W. W. Adams and E. I. Stiefel, *Science*, 1998, **282**, 1842–1843; R. Cammack, *Nature*, 1999, **397**, 214–215; M. Frey, *ChemBioChem*, 2002, **3**, 153–160.

2 J. W. Peters, W. N. Lanzilotta, B. J. Lemon and L. C. Seefeldt, *Science*, 1998, **282**, 1853–1858; B. J. Lemon and J. W. Peters, *Biochemistry*, 1999, **38**, 12969–12973; Y. Nicolet, C. Piras, P. Legrand, C. E. Hatchikian and J. C. Fontecilla-Camps, *Structure*, 1999, **7**, 13–23.

3 M. Schmidt, S. M. Contakes and T. B. Rauchfuss, *J. Am. Chem. Soc.*, 1999, **121**, 9736–9737; M. Y. Darensbourg, E. J. Lyon and J. J. Smee, *Coord. Chem. Rev.*, 2000, **206–207**, 533–561; L. C. Song, *Acc. Chem. Res.*, 2005, **38**, 21–28; J. F. Capon, F. Gloaguen, P. Schollhammer and J. Talarmin, *Coord. Chem. Rev.*, 2005, **249**, 1664–1676; J. F. Capon, F. Gloaguen, F. Y. Petillon, P. Schollhammer and J. Talarmin, *Coord. Chem. Rev.*, 2009, **253**, 1476–1494; F. Gloaguen and T. B. Rauchfuss, *Chem. Soc. Rev.*, 2009, **38**, 100–108.

4 D. J. Evans and C. J. Pickett, *Chem. Soc. Rev.*, 2003, **32**, 268–275; S. P. Best, *Coord. Chem. Rev.*, 2005, **249**, 1536–1554; X. M. Liu, S. K. Ibrahim, C. Tard and C. J. Pickett, *Coord. Chem. Rev.*, 2005, **249**, 1641–1652; C. Tard and C. J. Pickett, *Chem. Rev.*, 2009, **109**, 2245–2274; S. Tschierlei, S. Ott and R. Lomoth, *Energy Environ. Sci.*, 2011, **4**, 2340–2352.

5 L. C. Sun, B. Akermark and S. Ott, *Coord. Chem. Rev.*, 2005, **249**, 1653–1663; R. Lomoth and S. Ott, *Dalton Trans.*, 2009, 9952–9959; M. Wang, L. Chen, X. Q. Li and L. C. Sun, *Dalton Trans.*, 2011, **40**, 12793–12800; M. Wang, L. Chen and L. Sun, *Energy Environ. Sci.*, 2012, **5**, 6763–6778; F. Wang, W. G. Wang, H. Y. Wang, G. Si, C. H. Tung and L. Z. Wu, *ACS Catal.*, 2012, **2**, 407–416; P. Du and R. Eisenberg, *Energy Environ. Sci.*, 2012, **5**, 6012–6021.

6 A. P. S. Samuel, D. T. Co, C. L. Stern and M. R. Wasielewski, *J. Am. Chem. Soc.*, 2010, **132**, 8813–8815; L. C. Song, X. F. Liu, J. B. Ming, J. H. Ge, Z. J. Xie and Q. M. Hu, *Organometallics*, 2010, **29**, 610–617; D. Streich, Y. Astuti, M. Orlandi, L. Schwartz, R. Lomoth, L. Hammarstrom and S. Ott, *Chem.–Eur. J.*, 2010, **16**, 60–63; F. Wang, W. G. Wang, X. J. Wang, H. Y. Wang, C. H. Tung and L. Z. Wu, *Angew. Chem., Int. Ed.*, 2011, **50**, 3193–3197; W. G. Wang, T. B. Rauchfuss, L. Bertini and G. Zampella, *J. Am. Chem. Soc.*, 2012, **134**, 4525–4528.

7 H. M. Wen, Y. H. Wu, Y. Fan, L. Y. Zhang, C. N. Chen and Z. N. Chen, *Inorg. Chem.*, 2010, **49**, 2210–2221; H. M. Wen, Y. H. Wu, L. J. Xu, L. Y. Zhang, C. N. Chen and Z. N. Chen, *Dalton Trans.*, 2011, **40**, 6929–6938.

8 G. A. N. Felton, R. S. Glass, D. L. Lichtenberger and D. H. Evans, *Inorg. Chem.*, 2006, **45**, 9181–9184; V. Fourmond, P. A. Jacques, M. Fontecave and V. Artero, *Inorg. Chem.*, 2010, **49**, 10338–10347.

9 L. Schwartz, P. S. Singh, L. Eriksson, R. Lomoth and S. Ott, *C. R. Chim.*, 2008, **11**, 875–889; S. Kaur-Ghumaan, L. Schwartz, R. Lomoth, M. Stein and S. Ott, *Angew. Chem., Int. Ed.*, 2010, **49**, 8033–8036.

10 Y. Na, M. Wang, J. X. Pan, P. Zhang, B. Akermark and L. C. Sun, *Inorg. Chem.*, 2008, **47**, 2805–2810; P. Li, M. Wang, L. Chen, J. H. Liu, Z. B. Zhaoa and L. C. Sun, *Dalton Trans.*, 2009, 1919–1926; F. W. Huo, J. Hou, G. C. Chen, D. M. Guo and X. J. Peng, *Eur. J. Inorg. Chem.*, 2010, 3942–3951.

11 M. Irie and M. Mohri, *J. Org. Chem.*, 1988, **53**, 803–808; M. Irie and K. Uchida, *Bull. Chem. Soc. Jpn.*, 1998, **71**, 985–996; M. Irie, *Chem. Rev.*, 2000, **100**, 1685–1716.

12 K. Matsuda and M. Irie, *J. Photochem. Photobiol., C*, 2004, **5**, 169–182; H. Tian and S. J. Yang, *Chem. Soc. Rev.*, 2004, **33**, 85–97.

13 P. H.-M. Lee, C.-C. Ko, N. Zhu and V. W.-W. Yam, *J. Am. Chem. Soc.*, 2007, **129**, 6058–6059; M. T. Indelli, S. Carli, M. Ghirotti, C. Chiorboli, M. Ravaglia, M. Garavelli and F. Scandola, *J. Am. Chem. Soc.*, 2008, **130**, 7286–7299; V. W.-W. Yam, J. K.-W. Lee, C.-C. Ko and N. Zhu, *J. Am. Chem. Soc.*, 2009, **131**, 912–913.

14 M. N. Roberts, C. J. Carling, J. K. Nagle, N. R. Branda and M. O. Wolf, *J. Am. Chem. Soc.*, 2009, **131**, 16644–16645.

15 J. Ekstrom, M. Abrahamsson, C. Olson, J. Bergquist, F. B. Kaynak, L. Eriksson, S. C. Licheng, H. C. Becker, B. Akermark, L. Hammarstrom and S. Ott, *Dalton Trans.*, 2006, 4599–4606.

16 B. Li, Y. H. Wu, H. M. Wen, L. X. Shi and Z. N. Chen, *Inorg. Chem.*, 2012, **51**, 1933–1942.

17 R. Mejia-Rodriguez, D. S. Chong, J. H. Reibenspies, M. P. Soriaga and M. Y. Darensbourg, *J. Am. Chem. Soc.*, 2004, **126**, 12004–12014; Z. Wang, J. H. Liu, C. J. He, S. Jiang, B. Akermark and L. C. Sun, *J. Organomet. Chem.*, 2007, **692**, 5501–5507; W. M. Gao, J. Ekstrom, J. H. Liu, C. N. Chen, L. Eriksson, L. H. Weng, B. Akermark and L. C. Sun, *Inorg. Chem.*, 2007, **46**, 1981–1991.

18 G. Si, W. G. Wang, H. Y. Wang, C. H. Tung and L. Z. Wu, *Inorg. Chem.*, 2008, **47**, 8101–8111; W. G. Wang, H. Y. Wang, G. Si, C. H. Tung and L. Z. Wu, *Dalton Trans.*, 2009, 2712–2720; X. H. Zeng, Z. M. Li and X. M. Liu, *Electrochim. Acta*, 2010, **55**, 2179–2185; L. J. Wang, Z. Y. Xiao, X. Ru and X. M. Liu, *RSC Adv.*, 2011, **1**, 1211–1219; N. Wen, F. F. Xu, Y. A. Feng and S. W. Du, *J. Inorg. Biochem.*, 2011, **105**, 1123–1130.

19 F. Gloaguen, J. D. Lawrence, M. Schmidt, S. R. Wilson and T. B. Rauchfuss, *J. Am. Chem. Soc.*, 2001, **123**, 12518–12527; L. C. Song, Z. Y. Yang, H. Z. Bian, Y. Liu, H. T. Wang, X. F. Liu and Q. M. Hu, *Organometallics*, 2005, **24**, 6126–6135; S. Gao, J. L. Fan, S. Sun, X. J. Peng, X. Zhao and J. Hou, *Dalton Trans.*, 2008, 2128–2135; F. F. Xu, S. W. Du, Y. P. Liu, J. Hassan, J. Zhang and A. M. Bond, *Dalton Trans.*, 2011, **40**, 10907–10917; C. Gimbert-Suriñach, M. Bhadbhade and S. B. Colbran, *Organometallics*, 2012, **31**, 3480–3491.

20 Y. T. Si, C. B. Ma, M. Q. Hu, H. Chen, C. C. Chen and T. Q. Liu, *New J. Chem.*, 2007, **31**, 1448–1454; M. Q. Hu, H. M. Wen, C. B. Ma, N. Li, Q. Y. Yan, H. Chen and C. N. Chen, *Dalton Trans.*, 2010, **39**, 9484–9486.

21 S. J. Borg, T. Behrsing, S. P. Best, M. Razavet, X. M. Liu and C. J. Pickett, *J. Am. Chem. Soc.*, 2004, **126**, 16988–16999; S. J. Borg, M. I. Bondin, S. P. Best, M. Razavet, X. Liu and C. J. Pickett, *Biochem. Soc. Trans.*, 2005, **33**, 3–6; S. J. Borg, J. W. Tye, M. B. Hall and S. P. Best, *Inorg. Chem.*, 2007, **46**, 384–394.

22 S. J. Borg, S. K. Ibrahim, C. J. Pickett and S. P. Best, *C. R. Chim.*, 2008, **11**, 852–860.

23 D. S. Chong, I. P. Georgakaki, R. Mejia-Rodriguez, J. Samabria-Chinchilla, M. P. Soriaga and M. Y. Darensbourg, *Dalton Trans.*, 2003, 4158–4163.
24 M. N. Roberts, J. K. Nagle, J. G. Finden, N. R. Branda and M. O. Wolf, *Inorg. Chem.*, 2009, **48**, 19–21.
25 J. Shin, J. Bertoia, K. R. Czerwinski and C. Bae, *Green Chem.*, 2009, **11**, 1576–1580.
26 E. J. Lyon, I. P. Georgakaki, J. H. Reibenspies and M. Y. Darensbourg, *J. Am. Chem. Soc.*, 2001, **123**, 3268–3278.
27 M. Irie, T. Lifka, S. Kobatake and N. Kato, *J. Am. Chem. Soc.*, 2000, **122**, 4871.
28 A. D. Becke, *J. Chem. Phys.*, 1993, **98**, 5648–5652.
29 J. P. Perdew, K. Burke and M. Ernzerhof, *Phys. Rev. Lett.*, 1996, **77**, 3865–3868.
30 R. Bauernschmitt and R. Ahlrichs, *Chem. Phys. Lett.*, 1996, **256**, 454–464; M. E. Casida, C. Jamorski, K. C. Casida and D. R. Salahub, *J. Chem. Phys.*, 1998, **108**, 4439–4449; R. E. Stratmann, G. E. Scuseria and M. J. Frisch, *J. Chem. Phys.*, 1998, **109**, 8218–8224.
31 V. Barone, M. Cossi and J. Tomasi, *J. Chem. Phys.*, 1997, **107**, 3210–3221; M. Cossi, G. Scalmani, N. Rega and V. Barone, *J. Chem. Phys.*, 2002, **117**, 43–54.
32 M. Dolg, U. Wedig, H. Stoll and H. Preuss, *J. Chem. Phys.*, 1987, **86**, 866–872; P. Schwerdtfeger, M. Dolg, W. H. E. Schwarz, G. A. Bowmaker and P. D. W. J. Boyd, *Chem. Phys.*, 1989, **91**, 1762–1774; D. Andrae, U. Häussermann, M. Dolg, H. Stoll and H. Preuss, *Theor. Chim. Acta*, 1990, **77**, 123–141.
33 M. M. Francl, W. J. Pietro, W. J. Hehre, J. S. Binkley, M. S. Gordon, D. J. DeFrees and J. A. Pople, *J. Chem. Phys.*, 1982, **77**, 3654–3665.
34 A. W. Ehlers, M. Böhme, S. Dapprich, A. Gobbi, A. Höllwarth, V. Jonas, K. F. Köhler, R. Stegmann, A. Veldkamp and G. Frenking, *Chem. Phys. Lett.*, 1993, **208**, 111–114.
35 P. Pyykkő and F. Mendizabal, *Inorg. Chem.*, 1998, **37**, 3018–3025.
36 M. J. Frisch, G. W. Trucks, H. B. Schlegel, G. E. Scuseria, M. A. Robb, J. R. Cheeseman, J. A. Montgomery, Jr., T. Vreven, K. N. Kudin, J. C. Burant, J. M. Millam, S. S. Iyengar, J. Tomasi, V. Barone, B. Mennucci, M. Cossi, G. Scalmani, N. Rega, G. A. Petersson, H. Nakatsuji, M. Hada, M. Ehara, K. Toyota, R. Fukuda, J. Hasegawa, M. Ishida, T. Nakajima, Y. Honda, O. Kitao, H. Nakai, M. Klene, X. Li, J. E. Knox, H. P. Hratchian, J. B. V. Bakken, C. Adamo, J. Jaramillo, R. Gomperts, R. E. Stratmann, O. Yazyev, A. J. Austin, R. Cammi, C. Pomelli, J. W. Ochterski, P. Y. Ayala, K. Morokuma, G. A. Voth, P. Salvador, J. J. Dannenberg, V. G. Zakrzewski, S. Dapprich, A. D. Daniels, M. C. Strain, O. Farkas, D. K. Malick, A. D. Rabuck, K. Raghavachari, J. B. Foresman, J. V. Ortiz, Q. Cui, A. G. Baboul, S. Clifford, J. Cioslowski, B. B. Stefanov, G. Liu, A. Liashenko, P. Piskorz, I. Komaromi, R. L. Martin, D. J. Fox, T. Keith, M. A. Al-Laham, C. Y. Peng, A. Nanayakkara, M. Challacombe, P. M. W. Gill, B. Johnson, W. Chen, M. W. Wong, C. Gonzalez and J. A. Pople, *Gaussian 03, revision D.02*. Gaussian, Inc., Wallingford, CT, 2004.
37 P. Ros and G. C. A. Schuit, *Theor. Chim. Acta*, 1966, **4**, 1–12.